



Published in final edited form as:

*Cell Calcium*. 2012 September ; 52(3-4): 208–216. doi:10.1016/j.ceca.2012.06.004.

## Ca<sup>2+</sup> influx and neurotransmitter release at ribbon synapses

Soyoun Cho and Henrique von Gersdorff

The Vollum Institute, Oregon Health and Science University Portland, Oregon, 97239, USA

### Abstract

Ca<sup>2+</sup> influx through voltage-gated Ca<sup>2+</sup> channels triggers the release of neurotransmitters at presynaptic terminals. Some sensory receptor cells in the peripheral auditory and visual systems have specialized synapses that express an electron-dense organelle called a synaptic ribbon. Like conventional synapses, ribbon synapses exhibit SNARE-mediated exocytosis, clathrin-mediated endocytosis, and short-term plasticity. However, unlike non-ribbon synapses, voltage-gated L-type Ca<sup>2+</sup> channel opening at ribbon synapses triggers a form of multiquantal release that can be highly synchronous. Furthermore, ribbon synapses appear to be specialized for fast and high throughput exocytosis controlled by graded membrane potential changes. Here we will discuss some of the basic aspects of synaptic transmission at different types of ribbon synapses, and we will emphasize recent evidence that auditory and retinal ribbon synapses have marked differences. This will lead us to suggest that ribbon synapses are specialized for particular operating ranges and frequencies of stimulation. We propose that different types of ribbon synapses transfer diverse rates of sensory information by expressing a particular repertoire of critical components, and by placing them at precise and strategic locations, so that a continuous supply of primed vesicles and Ca<sup>2+</sup> influx leads to fast, accurate, and ongoing exocytosis.

### Keywords

ribbon synapses; calcium channels; exocytosis; synaptic transmission; transmitter release; short-term plasticity; calcium microdomains

### Introduction

The synapses between auditory hair cells and afferent fibers are the first chemical synapse where transmission of the signals involved in hearing starts. Hair cells in the cochlea detect graded sound wave signals and convert them into bioelectrical signals, namely the opening of Ca<sup>2+</sup> channels and exocytosis. Release of glutamate onto the afferent fibers then leads to excitatory synaptic currents (EPSCs) that depolarize the afferent fiber, thus triggering all-or-none spikes. A similar form of analog-to-digital conversion of sensory signals also occurs in the retina, where graded light and dark signals are detected in photoreceptors and eventually converted to all-or-none spikes at ganglion cell axons. This transduction and encoding of incoming sensory information seems to require ribbon synapses at the first excitatory synapse of the auditory and visual systems, and even at the second (bipolar cell) excitatory synapse of the retina. Unlike most neuronal synapses, the distinctive characteristics of hair cells, photoreceptors and retinal bipolar cells are that they are able to

© 2012 Elsevier Ltd. All rights reserved.

**Publisher's Disclaimer:** This is a PDF file of an unedited manuscript that has been accepted for publication. As a service to our customers we are providing this early version of the manuscript. The manuscript will undergo copyediting, typesetting, and review of the resulting proof before it is published in its final citable form. Please note that during the production process errors may be discovered which could affect the content, and all legal disclaimers that apply to the journal pertain.

manage both tonic and graded release of synaptic vesicles at ribbon-type active zones without the necessity of action potential firing.

## The molecular basis for $\text{Ca}^{2+}$ -dependent exocytosis at ribbon synapses

Specialized organelles, called synaptic ribbons, are found in auditory and vestibular hair cells as well as the lateral line of teleosts. Ribbon synapses are also present in photoreceptor terminals and bipolar cell terminals in the vertebrate retina, and in electroreceptors in some marine vertebrates. Ribbons are electron-dense discs that tether a halo of synaptic vesicles via fine filaments [1]. The shapes of ribbons are varied; some are spherical, ellipsoidal or bar shaped depending on cell type, species, and developmental stages (Figure 1) [2, 3]. Ribbons may play a role in delivering vesicles to release sites and they probably contribute to create conditions that favor prominent multivesicular release [4–6]. Previous studies show that hair cells and photoreceptors lacking a scaffolding protein called bassoon also lack ribbons anchored to their plasma membrane at active zones, and show severe deficits of synaptic transmission in the retina [7] and cochlear inner hair cells [8]. This suggests that the ribbons may be required for the fast and precise release of synaptic vesicles during the onset of a stimulus and for the continuous high-rate of release during the stimulus [9]. However, the exact role of the synaptic ribbons remains elusive since some non-ribbon (conventional) synapses, like mossy fibers in the cerebellum, also can release large amounts of vesicles in a fast and continuous manner [10].

Although ribbon synapses and non-ribbon synapses function differently, the molecular composition of ribbon synapses appears to be mostly conserved and similar to that of non-ribbon synapses. Syntaxins, SNAP25, and synaptobrevin/VAMP (the three core SNARE proteins) are found in hair cells [11, 12] and in the photoreceptors and bipolar cells [1]. However, some synaptic proteins are unique to ribbons, such as RIBEYE, a novel protein with homology to both a transcription repressor factor (CtBP2) and a NADH dehydrogenase [13]. RIBEYE has been used as a useful tool to specifically target the synaptic ribbon with fluorescence [14–17]. In addition, ribbon synapses lack certain proteins that are found in non-ribbon synapses, such as the synapsin family of proteins. Synapsins link vesicles to the actin cytoskeleton in non-ribbon synapses and they appear to be absent from ribbon synapses. Synaptotagmins 1 and 2, the main putative  $\text{Ca}^{2+}$ -sensitive mediators of fast and synchronous release in the brain have not been found in the adult cochlea [11], but are present in photoreceptors and some bipolar cells. Instead, otoferlin is the proposed  $\text{Ca}^{2+}$  sensor for exocytosis in adult cochlear hair cells [18, 19, 119], though it may also have a  $\text{Ca}^{2+}$ -dependent vesicle recruitment function [20, 119]. However, inner hair cells in adult hypothyroid rats, which apparently do not express otoferlin, still can release transmitter, so otoferlin's exact role is still under investigation [21, 22]. Recent studies have also shown that the expression of synaptotagmins in mammalian hair cells depends on their developmental stage [22]. In addition, hair cells lack complexins [23, 121], which are expressed in retinal ribbon synapses [24]. Therefore, the composition of ribbon synapses in hair cells differs remarkably from that in the retina, and from that of non-ribbon synapses, though there are also many fundamental similarities.

## $\text{Ca}^{2+}$ channels and spatial-temporal profile of $\text{Ca}^{2+}$ influx

The essential role of  $\text{Ca}^{2+}$  in triggering neurotransmitter release has been well established [25, 26]. Basically,  $\text{Ca}^{2+}$  influx through open voltage-gated  $\text{Ca}^{2+}$  channels located at the active zone of a presynaptic terminal triggers neurotransmitter release via synaptic vesicle exocytosis [27]. In conventional synapses, voltage-gated  $\text{Ca}^{2+}$  channels open when an action potential invades the presynaptic terminal and depolarizes the membrane potential. In

contrast, graded membrane potential changes in ribbon synapses trigger transmitter release without sodium-based action potentials.

Among several types of voltage-gated  $\text{Ca}^{2+}$  channels (L-, N-, P/Q-, T- and R-type), the P/Q-type channel and the N-type channels mainly control transmitter release at most CNS bouton-type synapses and at the neuromuscular junction [28]. However, at ribbon synapses, the L-type channel is instead critical for neurotransmitter release, though some hair cells show multiple  $\text{Ca}^{2+}$  channel types [29]. Interestingly,  $\text{Ca}^{2+}$  currents show a very negative voltage activation range and a rapid gating in hair cells [6, 30, 113, 114].  $\text{Ca}^{2+}$ -dependent inactivation of  $\text{Ca}^{2+}$  currents has been observed in frog and turtle auditory hair cells [6, 114].

The entry of  $\text{Ca}^{2+}$  through voltage-gated  $\text{Ca}^{2+}$  channels increases the intracellular  $\text{Ca}^{2+}$  concentration transiently in a spatially restricted “microdomain” of the active zone [31, 32]. The microdomain concept can explain the rapid onset and cessation of neurotransmitter release in fast synaptic transmission. In non-ribbon synapses, such as calyx of Held, the  $\text{Ca}^{2+}$  sensor for neurotransmitter release is thought to be positioned very close to these  $\text{Ca}^{2+}$  channels at some active zones, so that transmitter release occurs within less than a millisecond [33]. In fact, the delay between  $\text{Ca}^{2+}$  influx and the fusion of synaptic vesicles at different synapses can be as little as 60–350  $\mu\text{sec}$ . This suggests that  $\text{Ca}^{2+}$  diffuses less than 100 nm to trigger the exocytosis of synaptic vesicles [34–36]. Given the homeostatic  $\text{Ca}^{2+}$  handling mechanisms ( $\text{Ca}^{2+}$  pumps,  $\text{Ca}^{2+}$  exchangers and  $\text{Ca}^{2+}$  buffers) present within nerve terminals, free  $\text{Ca}^{2+}$  cannot diffuse great distances in the nerve terminal, unless all these mechanisms are saturated by large  $\text{Ca}^{2+}$  influx loads.

The microdomain model predicts the existence of temporally and spatially restricted increases of intracellular  $\text{Ca}^{2+}$ , so called  $\text{Ca}^{2+}$  hotspots. In hair cells, such  $\text{Ca}^{2+}$  hotspots have been detected along the basolateral membrane of the hair cell where ribbons are located [37–39], whereas regions distal from the ribbons show only small and slow increases of  $\text{Ca}^{2+}$  signals, which are not coupled with the stimulus (Figure 2 and 3). This tight temporal and spatial regulation of intracellular  $\text{Ca}^{2+}$  requires strong  $\text{Ca}^{2+}$  clearance mechanisms such as a variety of  $\text{Ca}^{2+}$  ATP-ase pumps and  $\text{Ca}^{2+}$  exchangers in addition to a large concentration of mobile  $\text{Ca}^{2+}$  buffers. Mobile  $\text{Ca}^{2+}$  buffers can reduce free  $\text{Ca}^{2+}$  at the synapse on a fast time scale by binding  $\text{Ca}^{2+}$  ions that enter the cell and then shuttling them away from the active zone [40]. In contrast, fixed  $\text{Ca}^{2+}$  buffers may prolong the duration of the  $\text{Ca}^{2+}$  transients after rapidly binding the free  $\text{Ca}^{2+}$  and then releasing it with a delay [41]. Mobile  $\text{Ca}^{2+}$  buffers such as calretinin and parvalbumin help to spatially restrict and localize free  $\text{Ca}^{2+}$  ions within the bullfrog saccular hair cell [42–44]. High concentration of an exogenous  $\text{Ca}^{2+}$  buffer (for example 10 mM BAPTA) greatly restricts the spread of  $\text{Ca}^{2+}$  to the presynaptic dense body area (Figure 3E). Nevertheless, large EPSCs can still be observed at the postsynaptic afferent fiber with relatively mild depolarizations of the hair cell (Figure 3F). This suggests that the  $\text{Ca}^{2+}$  rise underneath the ribbon is sufficient to trigger large EPSCs and transiently overwhelms the various  $\text{Ca}^{2+}$  pumps,  $\text{Ca}^{2+}$  buffers, and intracellular  $\text{Ca}^{2+}$  stores that function to remove cytoplasmic  $\text{Ca}^{2+}$ . Plasma membrane  $\text{Ca}^{2+}$  ATPases, Na/Ca exchangers, the sarcoplasmic-endoplasmic reticulum  $\text{Ca}^{2+}$  pumps (SERCAs), and  $\text{Ca}^{2+}$  uptake into mitochondria play important roles in  $\text{Ca}^{2+}$  removal at different ribbon-type synapses [37, 45–48].

## The $\text{Ca}^{2+}$ -sensor molecules for exocytosis at ribbon synapses

At the individual vesicle level, there are several steps that bring synaptic vesicles into close apposition with presynaptic  $\text{Ca}^{2+}$  channels. Vesicles do not traffic through the cytoplasm randomly and most synaptic vesicles in presynaptic terminals are not immediately available

for fusion. Cytoskeletal elements, such as actin, myosin and motor proteins, may play important roles in the transport of vesicles. The disassembly of the actin network may control the transit of vesicles from the reserve pool to the readily releasable pool and this process can be regulated by  $\text{Ca}^{2+}$  and ATP [49–51]. A complex of proteins, called the “exocyst” interacts with the cytoskeleton to target vesicles to the active zone. Rab-3 may regulate the alignment of vesicles in the docking area and assist in the displacement of n-sec-1 from syntaxin (this step is often called tethering). Then, syntaxin and SNAP25 bind to VAMP to form the core SNARE complex. This step “docks” a vesicle to the release site at the active zone, which contains the presynaptic  $\text{Ca}^{2+}$  channels.  $\text{Ca}^{2+}$  binding to the  $\text{Ca}^{2+}$  sensor for exocytosis is thought to cause vesicle fusion [52]. After vesicle fusion, cytoplasmic NSF/ $\alpha$ -SNAP are thought to dissociate the tight SNARE core complex so that vesicles and their associated membrane proteins can be recycled [50, 53]. However, there is recent evidence that vesicle release at ribbon synapses may use atypical processes in comparison with non-ribbon synapses. A convincing study has shown that the typical neuronal SNARE proteins, which are specifically cleaved by neurotoxins, do not seem to be involved in the exocytosis process of mouse inner hair cells [120]. It is possible that the structure of the SNARE core complex may be more dynamic and the SNARE complex may be less stable (or less tightly coupled) in hair cell ribbon synapses [121, 122]. This may permit a more continuous and higher fusion rate at hair cells, which are epithelial cells that are not derived from the neural crest during development, and thus may contain non-typical SNARE molecules.

Based on its ability to bind to  $\text{Ca}^{2+}$ , and to link  $\text{Ca}^{2+}$  influx and vesicle fusion, the best candidate  $\text{Ca}^{2+}$  sensor for transmitter release is synaptotagmin in non-ribbon synapses. Synaptotagmin is a vesicle membrane protein with two cytoplasmic  $\text{Ca}^{2+}$ -binding motifs, called C2 domains (the C2A and C2B domains) [54, 55]. Synaptotagmin 1 is thought to function as a  $\text{Ca}^{2+}$  sensor regulating the fast, phasic exocytosis of synaptic vesicles [55]. Despite incomplete information, synaptotagmin 2 seems functionally similar to synaptotagmin 1 [56, 57], but synaptotagmin 5–7, 10 appear to be related with asynchronous release of transmitter [56]. Synaptotagmin 4 is predominantly expressed postsynaptically and may function in the release of retrograde signals that enhance presynaptic release [58]. Synaptotagmin 1 has 5  $\text{Ca}^{2+}$  binding sites; the C2A domain binds 3  $\text{Ca}^{2+}$  ions and the C2B domain binds 2  $\text{Ca}^{2+}$  ions [59]. Both C2 domains have low intrinsic affinity for  $\text{Ca}^{2+}$ . The affinity for  $\text{Ca}^{2+}$  of C2 domains strongly increases into physiological ranges when the C2 domains bind to phospholipids in the plasma membrane. Under these phospholipid binding conditions, the overall  $\text{Ca}^{2+}$  affinity of the C2 domains increases up to 5000 fold ( $K_D = 5\text{--}50 \mu\text{M}$ ), because additional coordination sites for  $\text{Ca}^{2+}$  are probably provided by the negatively charged phospholipid headgroups [60, 61]. Other synaptic molecules binding with synaptotagmin, such as syntaxin, SNAP-25, and intracellular domains of the voltage-gated  $\text{Ca}^{2+}$  channel, also affect  $\text{Ca}^{2+}$ -binding affinity of C2 domains [62]. The  $\text{Ca}^{2+}$  binding affinities described above may be relative values rather than absolute, because they depend on the composition of the phospholipid membranes [60, 61]. Depending on the exact lipid composition of the fusion sites, the real  $\text{Ca}^{2+}$  affinities may vary by a factor of 2–4 [61]. A previous study measured the response time of the synaptotagmin C2 domain and demonstrated that the synaptotagmin C2A domains could respond rapidly to both increases and decreases in  $\text{Ca}^{2+}$  concentration, which was fast enough to fit known rates for  $\text{Ca}^{2+}$ -triggered vesicle fusion. They also showed that  $\text{Ca}^{2+}$  binding triggered synaptotagmin penetration into the membrane and led to a simultaneous binding to the SNARE complex [63].

The precise dependence of transmitter release on  $\text{Ca}^{2+}$  concentration varies among different synapses. However, in many non-ribbon synapses, a nonlinear relationship, such as a third to fourth order cooperative relationship, between  $\text{Ca}^{2+}$  concentration and transmitter release is

observed across various synapses and species, including the squid giant synapse [34, 64], the crayfish neuromuscular junction [65], the frog neuromuscular junction [26, 66], the calyx of Held [67, 68] and hippocampal CA3-CA1 synapses [69]. The number of  $\text{Ca}^{2+}$  channels that contribute to the release of a single vesicle also seems different among various synapses [33, 34, 70–72]. Two models have been proposed: the single-channel “nanodomain” hypothesis, which suggests that  $\text{Ca}^{2+}$  influx through a single  $\text{Ca}^{2+}$  channel triggers the release of a vesicle, and the “overlapping microdomain” hypothesis, which suggests that multiple  $\text{Ca}^{2+}$  channels contribute to the fusion of a single vesicle and overlapping  $\text{Ca}^{2+}$  microdomains are required to trigger release. Based on the non-linear dependence of transmitter release on  $\text{Ca}^{2+}$  entry, as well as the tight temporal and spatial relationship between  $\text{Ca}^{2+}$  and transmitter release, even slight modifications of presynaptic  $\text{Ca}^{2+}$  influx rates would be expected to significantly affect transmitter release.

While many non-ribbon synapses have shown a fourth order power-law dependence of release on  $\text{Ca}^{2+}$ , hair cell ribbon synapses have shown a linear or sublinear  $\text{Ca}^{2+}$  dependence of neurotransmitter release [73–77], and this changes depending on developmental maturation. A similar linear relationship between  $\text{Ca}^{2+}$  influx and transmitter release is also found at the photoreceptor synapse [78]. At hair cells this linear dependence may be due to the unique  $\text{Ca}^{2+}$  sensor, otoferlin, plus the presence of synaptotagmin 4, and to other isoforms of synaptotagmins at retinal ribbon synapses [22, 78]. A linear function may be expected if the exocytosis of a single vesicle is triggered by the  $\text{Ca}^{2+}$  influx through a single nearby  $\text{Ca}^{2+}$  channel, which results in no cooperativity among  $\text{Ca}^{2+}$  channels [79, 80]. However, recently, it has been proposed that this linearity may result from the summing across multiple active zones, which individually have a supralinear  $\text{Ca}^{2+}$  dependence of exocytosis [81].

### The number of $\text{Ca}^{2+}$ channels per synaptic ribbon

Voltage-gated  $\text{Ca}^{2+}$  channels are clustered at the synaptic ribbon active zone so that  $\text{Ca}^{2+}$  entry is highly localized to particular regions of the plasma membrane in mouse inner hair cells [15], and in frog [40] and turtle hair cells [37]. Importantly, the amplitude and voltage dependence of the individual  $\text{Ca}^{2+}$  microdomains vary considerably within a single mouse inner hair cell [15]. This suggests that the individual active zones may have different numbers of  $\text{Ca}^{2+}$  channels and this may lead to differences in transmitter release rates and spontaneous spike rates [15]. Freeze-fracture studies suggest that clusters of  $\text{Ca}^{2+}$  channels were located approximately 100 – 200 nm from the sites of exocytosis underneath the synaptic ribbon [116]. The total numbers of  $\text{Ca}^{2+}$  channel in hair cells are estimated to 1700 in mouse inner hair cells [79] and 2000 – 3000 in frog auditory hair cells [6]. The total number of  $\text{Ca}^{2+}$  channels in each active zone is about 90 in frog saccular hair cells [116] and about 80 in mouse cochlear inner hair cells [79]. Assuming that all  $\text{Ca}^{2+}$  channels are clustered close to ribbons, there are approximately 40 – 50  $\text{Ca}^{2+}$  channels per synaptic ribbon in frog auditory hair cells from the amphibian papilla [6]. The release of a single synaptic vesicle is regulated by only a few nearby  $\text{Ca}^{2+}$  channels [79]. In fact, the opening of a single  $\text{Ca}^{2+}$  channel may trigger the simultaneous release of up 5–6 vesicles (or quanta) at bullfrog hair cells, because large EPSC events were observed even when the hair cell was voltage-clamped to about  $-70$  mV, a membrane potential where very a few  $\text{Ca}^{2+}$  channels are open [6, 115].

### Vesicle pools and endocytosis at ribbon synapses

Synaptic vesicles belong to distinct releasable pools, which show different fusion competency as demonstrated by the multiple kinetic components of exocytosis [82]. This may result from different states of molecular readiness for exocytosis based on the



interaction of proteins participating in vesicle fusion. It may also reflect the physical distance of release sites (or docked vesicles) from  $\text{Ca}^{2+}$  channels [83, 84]. Although various synapses show a wide range in their ability to release neurotransmitter, most presynaptic terminals contain vesicles in a “readily releasable pool”, which can be released quickly upon stimulation. Vesicles in a large “reserve pool” are more reluctant and can only be mobilized more slowly in response to prolonged or strong stimulation. In addition, intermediate vesicle pools may contain vesicles released more slowly than vesicles of the readily releasable pool, but which can release faster than vesicles from the reserve pool. Some of these pools may correspond to morphologically defined vesicle pools. For example, synaptic vesicles docked to the presynaptic membrane appear to be the readily releasable pool at hippocampal synapses [85]. At ribbon synapses, the readily releasable pool can include vesicles tethered to the ribbons as well as the docked vesicles [6, 86, 87].

To maintain sustained release for prolonged periods of time, released vesicles should be quickly retrieved by endocytosis and eventually reloaded into vesicle pools [88]. Endocytosis is critical for synaptic function at non-ribbon synapses [89]. This process includes recovery of vesicle membrane after fusion, appropriate sorting of proteins needed for vesicle fusion, and refilling of neurotransmitter, all of which depend on temperature and developmental maturation [90]. It is still not clear how many different mechanisms for endocytosis exist in neurons. The fastest possible mode (a “kiss-and-run” type of vesicle cycling, also termed “flicker fusion”) suggests a fast closer of the fusion pore, and the refilling of empty vesicle sacs with neurotransmitter, after a transient fusion of the vesicle with the plasma membrane [91]. The slow pathway of endocytosis is generally thought to go through classical clathrin-mediated endocytosis [92]. It is uncertain how the different modes of endocytosis are chosen, how they depend on  $\text{Ca}^{2+}$ , and if clathrin-mediated endocytosis may be sufficiently fast at synapses to mediate most of the physiologically relevant endocytosis needed to maintain a steady nerve terminal and cellular surface area.

### Short-term plasticity at ribbon synapses

Physiological activity patterns lead to changes in synaptic strength at all types of synapses. Some synapses show increased neurotransmitter release with repeated stimulation, whereas other synapses a decrease in neurotransmitter release. These alterations in synaptic strength are often called “facilitation” for increases, or “depression” for decreases. The mechanisms that underlie these short-term processes may vary at different synapses, and the observed behavior is often a mix of the offsetting strengths of these influences. In general, at synapses with a high probability of release, depression dominates, while synapses with a low release probability tend to show facilitation [93]. While manipulating the release probability by changing the extracellular  $\text{Ca}^{2+}$  concentration can alter the form of short-term plasticity that dominates at a particular synapse, there are physiologically relevant manipulations that can change these plastic events as well. Possible physiologically relevant regulation sites for short-term synaptic plasticity include changes in the waveform of the presynaptic action potential [94], changes in  $\text{Ca}^{2+}$  influx [95], the size of the readily releasable pool [96], neuromodulators [97], and internal  $\text{Ca}^{2+}$  stores [98]. It is widely accepted that residual  $\text{Ca}^{2+}$  from previous stimulation causes activity-dependent synaptic facilitation, though the underlying molecular mechanisms of these dynamic changes in synaptic strength are not well understood. One possible mechanism for this is saturation of local  $\text{Ca}^{2+}$  buffers during the first action potential in a pair of stimuli [99]. In contrast, depletion of the vesicles within the readily releasable pool can cause synaptic depression [100]. In addition, postsynaptic receptors can be desensitized by a long exposure to neurotransmitter that reduces postsynaptic currents [101].

Many presynaptic proteins including synaptotagmin, synapsin, synaptophysin, and munc 13-1, and native  $\text{Ca}^{2+}$  binding proteins, such as frequenin and piccolo, can influence short-term plasticity [102–106]. Despite our current detailed molecular understanding of presynaptic events surrounding transmitter release, there is no general consensus as to the molecular mechanisms that underlie some of the particular phases of short-term plasticity. Much attention has been focused on trying to implicate various  $\text{Ca}^{2+}$  binding proteins found in synaptic terminals. As there are many mechanisms that may lead to short-term synaptic plasticity, at most synapses multiple mechanisms probably interact in complex ways to generate the plastic physiological patterns of synaptic transmission [107].

Interestingly, many ribbon synapses, such as retinal bipolar cells of the goldfish, rod bipolar cells in the rat retina, photoreceptors of salamanders, frog saccular hair cells and cochlear inner hair cells of the mouse, show only short-term depression (Figure 4). These studies used a variety of experimental stimulation protocols, such as different durations and amplitudes of depolarization, and different durations of inter-pulse intervals, external  $\text{Ca}^{2+}$  concentrations, internal  $\text{Ca}^{2+}$  buffers, and holding potentials [86, 87, 108–112]. So it is hard to compare the detailed results from all these different ribbon-type synapses.

Facilitation has been observed at ribbon synapses, namely in auditory hair cell synapses in rats [117], bullfrogs [77] and in the *in vivo* chinchilla auditory nerve fiber using sound stimuli [118]. In adult bullfrog amphibian papilla hair cells, the recovery rate from paired-pulse depression was surprisingly fast (about ten milliseconds; Figure 4A–D). A clear form of paired-pulse facilitation was also observed, although depression dominated with a longer depolarizing pulse duration [77]. Likewise, the recovery from paired-pulse depression in acutely isolated frog saccular hair cells is very fast with a time constant of 29 ms [110]. In chick hair cell synapses, sound-evoked adaptation quickly recovers ( $\tau = 70$  ms) [87], and a rapid calcium-dependent vesicle supply mechanism allows sustained high rates of exocytosis in more mature hair cells [119]. Mouse inner hair cells show a biphasic recovery ( $\tau_f = 140$  ms and  $\tau_s = 3$  s) from depletion of the readily releasable pool [108]. By contrast, goldfish retinal bipolar cell terminals show a relatively slow double-exponential recovery from paired-pulse depression ( $\tau_f = 1.03$  s and  $\tau_s = 11.8$  s; Figure 4F). Interestingly, the  $\text{Ca}^{2+}$  currents evoked by a pair of stimuli show facilitation in bipolar cell terminals (Figure 4E), whereas in hair cell ribbon synapses they show inactivation (Figure 4A). Recovery from paired-pulse depression in rat rod bipolar cell synapses is also relatively slow ( $\tau = 4$  s) [111].

In conclusion, several recent studies indicate that recovery from depression at auditory hair cell synapses is generally faster than at retinal ribbon synapses. Perhaps hair-cell synaptic ribbons, and their surrounding vesicle mobilization machinery, are tailored for fast and efficient replenishment of depleted vesicle pools, so that these synapses can transmit faithfully the phase-locked timing of high frequency sound signals [6, 77]. The remarkable speed and continuous release in the processing of ongoing auditory signals in hair cell synapses may require a fast and calcium-dependent recruitment of vesicles towards the synaptic ribbons and this results in a fast time course of recovery from depression. Such stringent requirements for speed and precise timing in the release process may not be necessary in the retinal ribbon synapses since visual signals are intrinsically slower and rate limited by the relatively slow phototransduction cascade in rods and cones [77]. Different ribbon synapses thus have remarkably different properties that seem to be tailored to their kinetic operating ranges and rate limited to match their respective physiological sensory transduction processes.

## References

1. Lenzi D, von Gersdorff H. Structure suggests function: the case for synaptic ribbons as exocytotic nanomachines. *Bioessays*. 2001; 23:831–840. [PubMed: 11536295]
2. Liberman MC. Morphological differences among radial afferent fibers in the cat cochlea: an electron-microscopic study of serial sections. *Hear Res*. 1980; 3:45–63. [PubMed: 7400048]
3. Neef A, Khimich D, Pirih P, Riedel D, Wolf F, Moser T. Probing the mechanism of exocytosis at the hair cell ribbon synapse. *J Neurosci*. 2007; 27:12933–12944. [PubMed: 18032667]
4. von Gersdorff H. Synaptic ribbons: versatile signal transducers. *Neuron*. 2001; 29:7–10. [PubMed: 11182076]
5. Parsons TD, Sterling P. Synaptic ribbon: Conveyor belt or safety belt? *Neuron*. 2003; 37:379–382. [PubMed: 12575947]
6. Graydon CW, Cho S, Li GL, Kachar B, von Gersdorff H H. Sharp  $\text{Ca}^{2+}$  nanodomains beneath the ribbon promote highly synchronous multivesicular release at hair cell synapses. *J Neurosci*. 2011; 31:16637–16650. [PubMed: 22090491]
7. Dick O, tom Dieck S, Altmann WD, et al. The presynaptic active zone protein bassoon is essential for photoreceptor ribbon synapse formation in the retina. *Neuron*. 2003; 37:775–786. [PubMed: 12628168]
8. Khimich D, Nouvian R, Pujol R, et al. Hair cell synaptic ribbons are essential for synchronous auditory signaling. *Nature*. 2005; 434:889–894. [PubMed: 15829963]
9. Buran BN, Strenzke N, Neef A, Gundelfinger ED, Moser T, Liberman MC. Onset coding is degraded in auditory nerve fibers from mutant mice lacking synaptic ribbons. *J Neurosci*. 2010; 30:7587–7597. [PubMed: 20519533]
10. Saviane C, Silver RA. Fast vesicle reloading and a large pool sustain high bandwidth transmission at a central synapse. *Nature*. 2006; 439:983–987. [PubMed: 16496000]
11. Safieddine S, Wenthold RJ. SNARE complex at the ribbon synapses of cochlear hair cells: analysis of synaptic vesicle- and synaptic membrane-associated proteins. *Eur J Neurosci*. 1999; 11:803–812. [PubMed: 10103074]
12. Uthaiyah RC, Hudspeth AJ. Molecular anatomy of the hair cell's ribbon synapse. *J Neurosci*. 2010; 30:12387–12399. [PubMed: 20844134]
13. Schmitz F, Königstorfer A, Südhof TC. RIBEYE, a component of synaptic ribbons: a protein's journey through evolution provides insight into synaptic ribbon function. *Neuron*. 2000; 28:857–872. [PubMed: 11163272]
14. Zenisek D, Horst NK, Merrifield C, Sterling P, Matthews G. Visualizing synaptic ribbons in the living cell. *J Neurosci*. 2004; 24:9752–9759. [PubMed: 15525760]
15. Frank T, Khimich D, Neef A, Moser T. Mechanisms contributing to synaptic  $\text{Ca}^{2+}$  signals and their heterogeneity in hair cells. *PNAS*. 2009; 106:4483–4488. [PubMed: 19246382]
16. Bartoletti TM, Babai N, Thoreson WB. Vesicle pool size at the salamander cone ribbon synapse. *J Neurophysiol*. 2010; 103:419–423. [PubMed: 19923246]
17. Snellman J, Mehta B, Babai N, et al. Acute destruction of the synaptic ribbon reveals a role for the ribbon in vesicle priming. *Nat. Neurosci*. 2011; 14:1135–1141. [PubMed: 21785435]
18. Roux I, Safieddine S, Nouvian R, et al. Otoferlin, defective in a human deafness form, is essential for exocytosis at the auditory ribbon synapse. *Cell*. 2006; 127:277–289. [PubMed: 17055430]
19. Beurg M, Safieddine S, Roux I, Bouleau Y, Petit C, Dulon D. Calcium- and otoferlin-dependent exocytosis by immature outer hair cells. *J Neurosci*. 2008; 28:1798–1803. [PubMed: 18287496]
20. Pangrsic T, Lasarow L, Reuter K, et al. Hearing requires otoferlin-dependent efficient replenishment of synaptic vesicles in hair cells. *Nat Neurosci*. 2010; 13:869–876. [PubMed: 20562868]
21. Brandt N, Kuhn S, Munkner S, et al. Thyroid hormone deficiency affects postnatal spiking activity and expression of  $\text{Ca}^{2+}$  and  $\text{K}^{+}$  channels in rodent inner hair cells. *J Neurosci*. 2007; 27:3174–3186. [PubMed: 17376979]
22. Johnson SL, Franz C, Kuhn S, et al. Synaptotagmin IV determines the linear  $\text{Ca}^{2+}$  dependence of vesicle fusion at auditory ribbon synapses. *Nat. Neurosci*. 2010; 13:45–52. [PubMed: 20010821]



23. Strenzke N, Chanda S, Kopp-Scheinflug C, et al. Complexin-I is required for high-fidelity transmission at the endbulb of held auditory synapse. *J Neurosci.* 2009; 29:7991–8004. [PubMed: 19553439]
24. Reim K, Wegmeyer H, Brandstatter JH, et al. Structurally and functionally unique complexins at retinal ribbon synapses. *J Cell Biol.* 2005; 169:669–680. [PubMed: 15911881]
25. Katz B, Miledi R. The effect of calcium on acetylcholine release from motor nerve terminals. *Proceedings of the Royal Society of London, Series B, Biological Sciences.* 1965; 161:496–503.
26. Dodge FA Jr, Rahamimoff R. Co-operative action of calcium ions in transmitter release at the neuromuscular junction. *J Physiol.* 1967; 193:419–432. [PubMed: 6065887]
27. Augustine GJ, Charlton MP, Smith SJ. Calcium action in synaptic transmitter release. *Annu. Rev. Neurosci.* 1987; 10:633–693. [PubMed: 2436546]
28. Meir A, Ginsburg S, Butkevich A, et al. Ion channels in presynaptic nerve terminals and control of transmitter release. *Physiol Rev.* 1999; 79:1019–1088. [PubMed: 10390521]
29. Rennie KJ, Ashmore JF. Ionic currents in isolated vestibular hair cells from the guinea-pig crista ampullaris. *Hearing Res.* 1991; 51:279–291.
30. Rodriguez-Contreras A, Yamoah EN. Direct measurement of single-channel  $\text{Ca}^{2+}$  currents in bullfrog hair cells reveals two distinct channel subtypes. *J Physiol.* 2001; 534:669–689. [PubMed: 11483699]
31. Llinas R, Moreno H. Local calcium signaling in neurons. *Cell Calcium.* 1998; 24:359–366. [PubMed: 10091005]
32. Schneggenburger R, Neher E. Presynaptic calcium and control of vesicle fusion. *Curr Opin Neurobiol.* 2005; 15:266–274. [PubMed: 15919191]
33. Borst JGG, Sakmann B. Calcium influx and transmitter release in a fast CNS synapse. *Nature.* 1996; 383:431–434. [PubMed: 8837774]
34. Llinas R, Steinberg IZ, Walton K. Relationship between presynaptic calcium current and postsynaptic potential in squid giant synapse. *Biophys J.* 1981; 33:323–351. [PubMed: 6261850]
35. Heidelberger R, Heinemann C, Neher E, Matthews G. Calcium dependence of the rate of exocytosis in a synaptic terminal. *Nature.* 1994; 371:513–515. [PubMed: 7935764]
36. Heidelberger R, von Gersdorff H. Illuminating the calcium sensor for exocytosis in a flash. *Nature Neuroscience.* 2005; 8:402–404.
37. Tucker T, Fettiplace R. Confocal imaging of calcium microdomains and calcium extrusion in turtle hair cells. *Neuron.* 1995; 15:1323–1335. [PubMed: 8845156]
38. Rispoli G, Martini M, Rossi ML, Mammano F. Dynamics of intracellular calcium in hair cells isolated from the semicircular canal of the frog. *Cell Calcium.* 2001; 30:131–140. [PubMed: 11440470]
39. Schnee ME, Santos-Sacchi J, Castellano-Munoz M, Kong J, Ricci AJ. Calcium-dependent synaptic vesicle trafficking underlies indefatigable release at the hair cell afferent fiber synapse. *Neuron.* 2011; 70:326–338. [PubMed: 21521617]
40. Issa NP, Hudspeth AJ. The entry and clearance of Ca at individual presynaptic active zones of hair cells from the bullfrog's sacculus. *PNAS.* 1996; 93:9527–9532. [PubMed: 8790364]
41. Neher E, Augustine GJ. Calcium gradients and buffers in bovine chromaffin cells. *J Physiol.* 1992; 450:273–301. [PubMed: 1331424]
42. Roberts WM. Spatial calcium buffering in saccular hair cells. *Nature.* 1993; 363:74–76. [PubMed: 8479539]
43. Edmonds BW, Reyes R, Schwaller B, Roberts WM. Calcitonin modifies presynaptic calcium signaling in frog saccular hair cells. *Nat Neurosci.* 2000; 3:786–790. [PubMed: 10903571]
44. Heller S, Bell AM, Denis CS, Choe Y, Hudspeth AJ. Parvalbumin 3 is an abundant  $\text{Ca}^{2+}$  buffer in hair cells. *JARO.* 2002; 3:488–498. [PubMed: 12072915]
45. Carafoli E. The plasma membrane calcium pump in the hearing process: physiology and pathology. *Sci China Life Sci.* 2011; 54:686–690. [PubMed: 21786191]
46. Mulkey RM, Zucker RS. Monensin can transport calcium across cell membranes in a sodium independent fashion in the crayfish, *Procambarus clarkii*. *Neurosci Lett.* 1992; 143:115–118. [PubMed: 1436653]

47. Yamoah EN, Lumpkin EA, Dumont RA, Smith PJ, Hudspeth AJ, Gillespie PG. Plasma membrane  $\text{Ca}^{2+}$ -ATPase extrudes  $\text{Ca}^{2+}$  from hair cell stereocilia. *J Neurosci*. 1998; 18:610–624. [PubMed: 9425003]
48. Zenisek D, Matthews G. The role of mitochondria in presynaptic calcium handling at a ribbon synapse. *Neuron*. 2000; 25:229–237. [PubMed: 10707986]
49. Prekeris R, Terrian DM. Brain myosin V is a synaptic vesicle-associated motor protein: evidence for a calcium-dependent interaction with the synaptobrevin-synaptophysin complex. *J Cell Biol*. 1997; 137:1589–1601. [PubMed: 9199173]
50. Bajjalieh SM. Synaptic vesicle docking and fusion. *Curr Opin Neurobiol*. 1999; 9:321–328. [PubMed: 10395572]
51. Srinivasan G, Kim J-H, von Gersdorff H. The pool of fast releasing vesicles is augmented by myosin light chain kinase inhibition at the calyx of Held synapse. *J Neurophysiol*. 2008; 99:1810–1824. [PubMed: 18256166]
52. Martens S, Kozlov M, McMahon HT. How synaptotagmin promotes membrane fusion. *Science*. 2007; 316:1205–1208. [PubMed: 17478680]
53. Chapman ER. Synaptotagmin: A  $\text{Ca}^{2+}$  sensor that triggers exocytosis? *Nat Rev Mol Cell Biol*. 2002; 3:498–508. [PubMed: 12094216]
54. Perin MS, Fried VA, Mignery GA, Jahn R, Sudhof TC. Phospholipid binding by a synaptic vesicle protein homologous to the regulatory region of protein kinase C. *Nature*. 1990; 345:260–263. [PubMed: 2333096]
55. Geppert M M, Archer III BT, Sudhof TC. Synaptotagmin II: a novel differentially distributed form of synaptotagmin. *J Biol Chem*. 1991; 266:13548–13552. [PubMed: 1856191]
56. Hui E, Bai J, Wang P, Sugimori M, Llinas RR, Chapman ER. Three distinct kinetic groupings of the synaptotagmin family: Candidate sensors for rapid and delayed exocytosis. *PNAS*. 2005; 102:5210–5214. [PubMed: 15793006]
57. Xu J, Mashimo T, Sudhof TC. Synaptotagmin-1-2, and -9:  $\text{Ca}^{2+}$  sensors for fast release that specify distinct presynaptic properties in subsets of neurons. *Neuron*. 2007; 54:567–581. [PubMed: 17521570]
58. Adolfsen B, Saraswati S, Yoshihara M, Littleton JT. Synaptotagmins are trafficked to distinct subcellular domains including the postsynaptic compartments. *J Cell Biol*. 2004; 166:249–260. [PubMed: 15263020]
59. Fernandez I, Arac D, Ubach J, et al. Three-dimensional structure of the synaptotagmin 1 C2B-domain: synaptotagmin I as a phospholipid-binding module. *Neuron*. 2001; 32:1057–1069. [PubMed: 11754837]
60. Fernandez-Chacon R, Konigstorfer A, Gerber SH SH, et al. Synaptotagmin I functions as a calcium regulator of release probability. *Nature*. 2001; 410:41–49. [PubMed: 11242035]
61. Sugita S, Shin OH, Han W, Lao Y, Sudhof TC. Synaptotagmins form a hierarchy of exocytotic  $\text{Ca}^{2+}$  sensors with distinct  $\text{Ca}^{2+}$  affinities. *EMBO J*. 2002; 21:270–280. [PubMed: 11823420]
62. Chapman ER, Desai RC, Davis AF, Tornehl CK. Delineation of the oligomerization, AP-2 binding, and synprint binding region of the C2B domain of synaptotagmin. *J Biol Chem*. 1998; 273:32966–32972. [PubMed: 9830048]
63. Davis AF, Bai J, Fasshauer D, Wolowick MJ, Lewis JL, Chapman ER. Kinetics of synaptotagmin responses to  $\text{Ca}^{2+}$  and assembly with the core SNARE complex onto membranes. *Neuron*. 1999; 24:363–376. [PubMed: 10571230]
64. Augustine GJ, Charlton MP, Smith SJ. Calcium entry and transmitter release at voltage-clamped nerve terminals of squid. *J Physiol*. 1985; 367:163–181. [PubMed: 2865362]
65. Dudel J. The effect of reduced calcium on quantal unit current and release at the crayfish neuromuscular junction. *Pflugers Archiv – Eur J Physiol*. 1981; 391:35–40. [PubMed: 6269044]
66. Barton SB, Cohen IS, Van der Kloot W. The calcium dependence of spontaneous and evoked quantal release at the frog neuromuscular junction. *J Physiol*. 1983; 337:735–751. [PubMed: 6603514]
67. Barnes-Davis M, Forsythe ID. Pre- and postsynaptic glutamate receptors at a giant excitatory synapse in rat auditory brainstem slices. *J Physiol*. 1995; 488:387–406. [PubMed: 8568678]

68. Schneggenburger R, Neher E. Intracellular calcium dependence of transmitter release rates at a fast central synapse. *Nature*. 2000; 406:889–893. [PubMed: 10972290]
69. Wu LG, Saggau P. Presynaptic calcium is increased during normal synaptic transmission and paired-pulse facilitation, but not in long-term potentiation in area CA1 of hippocampus. *J Neurosci*. 1994; 14:645–654. [PubMed: 7905515]
70. Adler EM, Augustine GJ, Duffy SD, Charlton MP. Alien intracellular calcium chelators attenuate neurotransmitter release at the squid giant synapse. *J Neurosci*. 1991; 11:1496–1507. [PubMed: 1675264]
71. Stanley EF. Single calcium channels and acetylcholine release at a presynaptic nerve terminal. *Neuron*. 1993; 11:1007–1011. [PubMed: 8274272]
72. Fedchyshyn MJ, Wang LY. Developmental transformation of the release modality at the calyx of Held synapse. *J Neurosci*. 2005; 25:4131–4140. [PubMed: 15843616]
73. Johnson SL, Marcotti W, Kros CJ. Increase in efficiency and reduction in  $\text{Ca}^{2+}$  dependence of exocytosis during development of mouse inner hair cells. *J Physiol*. 2005; 563:177–191. [PubMed: 15613377]
74. Johnson SL, Forge A, Knipper M, Munkner S, Marcotti W. Tonotopic variation in the calcium dependence of neurotransmitter release and vesicle pool replenishment at mammalian auditory ribbon synapses. *J Neurosci*. 2008; 28:7670–7678. [PubMed: 18650343]
75. Keen EC, Hudspeth AJ. Transfer characteristics of the hair cell's afferent synapse. *PNAS*. 2006; 103:5537–5542. [PubMed: 16567618]
76. Goutman JD, Glowatzki E. Time course and calcium dependence of transmitter release at a single ribbon synapse. *PNAS*. 2007; 104:16341–16346. [PubMed: 17911259]
77. Cho S, Li GL, von Gersdorff H. Recovery from short-term depression and facilitation is ultrafast and  $\text{Ca}^{2+}$  dependent at auditory hair cell synapses. *J Neurosci*. 2011; 31:5682–5692. [PubMed: 21490209]
78. Thoreson WB, Rabl K, Townes-Anderson E, Heidelberger R. A highly  $\text{Ca}^{2+}$ -sensitive pool of vesicles contributes to linearity at the rod photoreceptor ribbon synapse. *Neuron*. 2004; 42:595–605. [PubMed: 15157421]
79. Brandt A, Khimich D, Moser T. Few  $\text{Ca}_v1.3$  channels regulate the exocytosis of a synaptic vesicle at the hair cell ribbon synapse. *J Neurosci*. 2005; 25:11577–11585. [PubMed: 16354915]
80. Jarsky T, Tian M, Singer JH. Nanodomain control of exocytosis is responsible for the signaling capability of a retinal ribbon synapse. *J Neurosci*. 2010; 30:11885–11895. [PubMed: 20826653]
81. Heil P, Neubauer H. Summing across different active zones can explain the quasi-linear calcium dependencies of exocytosis by receptor cells. *Front. Syn. Neurosci*. 2010; 2:148.
82. von Gersdorff H, Matthews G. Dynamics of synaptic vesicle fusion and membrane retrieval in synaptic terminals. *Nature*. 1994; 367:735–739. [PubMed: 7906397]
83. Parsons TD, Ellis-Davies GC, Almers W. Millisecond studies of calcium-dependent exocytosis in pituitary melanotrophs: comparison of the photolabile calcium chelators nitrophenyl-EGTA and DM-nitrophen. *Cell Calcium*. 1996; 19:185–192. [PubMed: 8732258]
84. von Gersdorff H, Vardi E, Matthews G, Sterling P. Evidence that vesicles on the synaptic ribbon of retinal bipolar neurons can be rapidly released. *Neuron*. 1996; 16:1221–1227. [PubMed: 8663998]
85. Schikorski T, Stevens CF. Morphological correlates of functionally defined synaptic vesicle populations. *Nat Neurosci*. 2001; 4:391–395. [PubMed: 11276229]
86. Mennerick S, Matthews G. Ultrafast exocytosis elicited by calcium currents in synaptic terminals of retinal bipolar neurons. *Neuron*. 1996; 17:1241–1249. [PubMed: 8982170]
87. Spassova MA, Avissar M, Furman AC, Crumling MA, Saunders JC, Parsons TD. Evidence that rapid vesicle replenishment of the synaptic ribbon mediates recovery from short-term adaptation at the hair cell afferent synapse. *J Assoc Res Otolaryngol*. 2004; 5:376–390. [PubMed: 15675002]
88. Stevens CF. Neurotransmitter release at central synapses. *Neuron*. 2003; 40:381–388. [PubMed: 14556715]
89. Koenig JH, Kosaka T, Ikeda K. The relationship between the number of synaptic vesicles and the amount of transmitter released. *J Neurosci*. 1989; 9:1937–1942. [PubMed: 2566663]

90. Renden R, von Gersdorff H. Synaptic vesicle endocytosis at a CNS nerve terminal: faster kinetics at physiological temperatures and increased endocytotic capacity during maturation. *J Neurophysiol.* 2007; 98:3349–3359. [PubMed: 17942618]
91. Zhang Q, Li Y, Tsien RW. The dynamic control of kiss-and-run and vesicular reuse probed with single nanoparticles. *Science.* 2009; 323:1448–1453. [PubMed: 19213879]
92. Smith SM, Renden R, von Gersdorff H. Synaptic vesicle endocytosis: fast and slow modes of membrane retrieval. *Trends Neurosci.* 2008; 31:559–568. [PubMed: 18817990]
93. Thomson AM. Facilitation, augmentation and potentiation at central synapses. *Trends Neurosci.* 2000; 23:305–312. [PubMed: 10856940]
94. Taschenberger H, von Gersdorff H. Fine-tuning an auditory synapse for speed and fidelity: developmental changes in presynaptic waveform, EPSC kinetics, and synaptic plasticity. *J Neurosci.* 2000; 20:9162–9173. [PubMed: 11124994]
95. Borst JG, Sakmann B. Facilitation of presynaptic calcium currents in the rat brainstem. *J Physiol.* 1998; 513:149–155. [PubMed: 9782166]
96. Ryan TA, Smith SJ. Vesicle pool mobilization during action potential firing at hippocampal synapses. *Neuron.* 1995; 14:983–989. [PubMed: 7748565]
97. Stefani A, Pisani A, Mercuri NB, Calabresi P. The modulation of calcium currents by the activation of mGluRs: functional implications. *Mol Neurobiol.* 1996; 13:81–95. [PubMed: 8892337]
98. Levy M, Faas GC, Saggau P, Craigen WJ, Sweatt JD. Mitochondrial regulation of synaptic plasticity in the hippocampus. *J Biol Chem.* 2003; 278:17727–17734. [PubMed: 12604600]
99. Klingauf J, Neher E. Modeling buffered Ca diffusion near the membrane: implications for secretion in neuroendocrine cells. *Biophys J.* 1997; 72:674–690. [PubMed: 9017195]
100. von Gersdorff H, Matthews G. Depletion and replenishment of vesicle pools at a ribbon-type synaptic terminal. *J Neurosci.* 1997; 17:1919–1927. [PubMed: 9045721]
101. Trussell LO, Fischbach GD. Glutamate receptor desensitization and its role in synaptic transmission. *Neuron.* 1989; 3:209–218. [PubMed: 2576213]
102. Rivoecchi R, Pongs O, Theil T, Mallart A. Implication of frequenin in the facilitation of transmitter release in *Drosophila*. *J Physiol.* 1994; 474:223–232. [PubMed: 7911829]
103. Rosahl TW, Spillane D, Missler M, et al. Essential functions of synapsins I and II in synaptic vesicle regulation. *Nature.* 1995; 375:488–493. [PubMed: 7777057]
104. Ryan TA, Li L, Chin LS, Greengard P, Smith SJ. Synaptic vesicle recycling in synapsin I knockout mice. *J Cell Biol.* 1996; 134:1219–1227. [PubMed: 8794863]
105. Stevens CF, Wesseling JF. Augmentation is a potentiation of the exocytotic process. *Neuron.* 1999; 22:139–146. [PubMed: 10027296]
106. Gerber SH, Garcia J, Rizo J, Sudhof TC. An unusual C2-domain in the active-zone protein piccolo: implications for Ca<sup>2+</sup> regulation of neurotransmitter release. *EMBO J.* 2001; 20:1605–1619. [PubMed: 11285225]
107. von Gersdorff H, Borst JGG. Short-term plasticity at the calyx of Held. *Nature Rev Neurosci.* 2002; 3:53–64. [PubMed: 11823805]
108. Moser T, Beutner D. Kinetics of exocytosis and endocytosis at the cochlear inner hair cell afferent synapse of the mouse. *PNAS.* 2000; 97:883–888. [PubMed: 10639174]
109. Palmer MJ, Hull C, Vigh J, von Gersdorff H. Synaptic cleft acidification and modulation of short-term depression by exocytosed protons in retinal bipolar cells. *J Neurosci.* 2003; 23:11332–11341. [PubMed: 14672997]
110. Edmonds BW, Gregory FD, Schweizer FE. Evidence that fast exocytosis can be predominantly mediated by vesicles not docked at active zones in frog saccular hair cells. *J Physiol.* 2004; 560:439–450. [PubMed: 15308677]
111. Singer JH, Diamond JS. Vesicle depletion and synaptic depression at a mammalian ribbon synapse. *J Neurophysiol.* 2006; 95:3191–3198. [PubMed: 16452253]
112. Rabl K, Cadetti L, Thoreson WB. Paired-pulse depression at photoreceptor synapses. *J Neurosci.* 2006; 26:2555–2563. [PubMed: 16510733]

113. Beutner D, Moser T. The presynaptic function of mouse cochlear inner hair cells during development of hearing. *J Neurosci*. 2001; 21:4593–4599. [PubMed: 11425887]
114. Schnee ME, Ricci AJ. Biophysical and pharmacological characterization of voltage-gated calcium currents in turtle auditory hair cells. *J Physiol*. 2003; 549:697–717. [PubMed: 12740421]
115. Li G-L, Keen E, Andor-Ardo D, Hudspeth AJ, von Gersdorff H. The unitary event underlying multiquantal EPSCs at a hair cell's ribbon synapse. *J Neurosci*. 2009; 29:7558–7568. [PubMed: 19515924]
116. Roberts WM, Jacobs RA, Hudspeth AJ. Colocalization of ion channels involved in frequency selectivity and synaptic transmission at presynaptic active zones of hair cells. *J Neurosci*. 1990; 10:3664–3684. [PubMed: 1700083]
117. Goutman JD, Glowatzki E. Short-term facilitation modulates size and timing of the synaptic response at the inner hair cell ribbon synapse. *J Neurosci*. 2011; 31:7974–7981. [PubMed: 21632919]
118. Siegel JH, Relkin EM. Evidence for presynaptic facilitation in primary cochlear afferent neurons. *Hearing Research*. 1987; 29:169–177. [PubMed: 3624081]
119. Levic S, Bouleau Y, Dulon D. Developmental acquisition of a rapid calcium-regulated vesicle supply allows sustained high rates of exocytosis in auditory hair cells. *PLoS One*. 2011; 6:e25714. [PubMed: 21998683]
120. Nouvian R, Neef J, Bulankina AV, et al. Exocytosis at the hair cell ribbon synapse apparently operates without neuronal SNARE proteins. *Nat Neurosci*. 2011; 14:411–413. [PubMed: 21378973]
121. An SJ, Grabner CP, Zenisek D. Real-time visualization of complexin during single exocytic events. *Nat Neurosci*. 2010; 13:577–583. [PubMed: 20383135]
122. Montana V, Liu W, Mohideen U, Parpura V. Single molecule measurements of mechanical interactions within ternary SNARE complexes and dynamics of their disassembly: SNAP25 vs. SNAP 23. *J Physiol*. 2009; 587.9:1943–1960. [PubMed: 19273577]



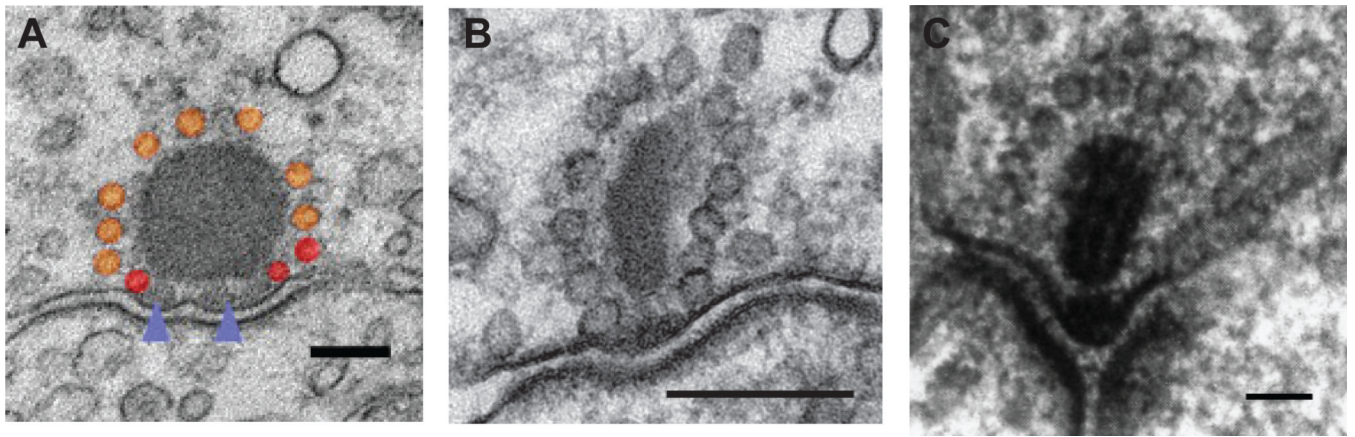


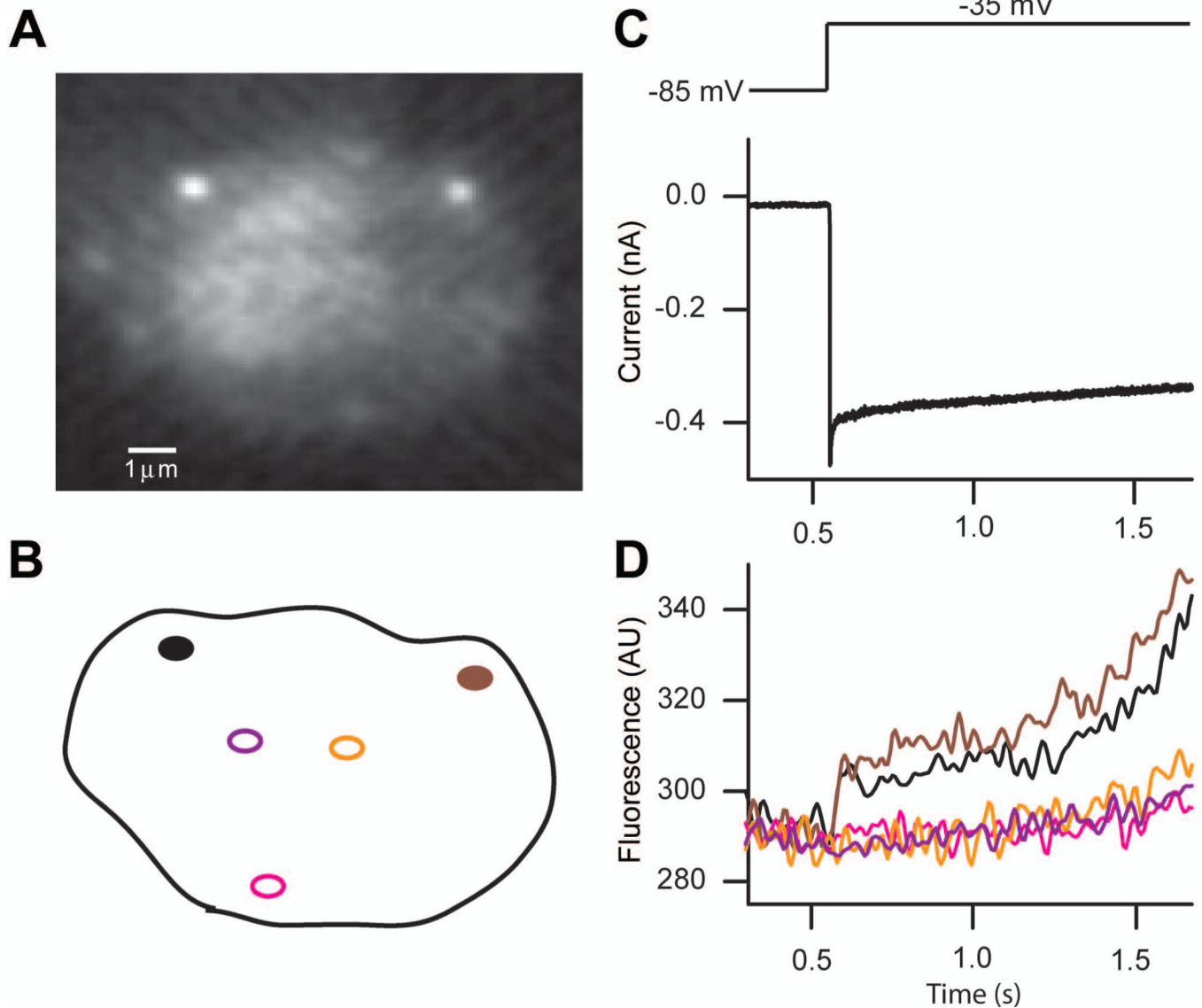
**Figure 1.**

Morphology of ribbon synapses. A halo of synaptic vesicles surround the electron dense synaptic ribbon. The ribbon can be plate-like, ellipsoidal, or spherical.

**A.** Representative section of adult bullfrog amphibian papilla hair cell synapse imaged at 40000 $\times$  (scale bar, 100 nm). Ribbon-attached vesicles (orange), immediately-releasable vesicles (red; vesicles docked on the membrane), ribbon anchoring sites (purple arrowheads). Modified with permission from Graydon et al., 2011 [6].

**B.** A mature (p14 – 17) mouse inner hair cell synapse (scale bar, 200 nm) viewed by electron microscopy. Modified from Neef et al., 2007 [3].

**C.** Ultrastructure of goldfish retina bipolar cell synapse (scale bar, 50 nm). The arciform density resides below the base of the synaptic ribbon. Modified from von Gersdorff et al., 1996 [84].

**Figure 2.**

High-speed confocal  $\text{Ca}^{2+}$  imaging of presynaptic dense bodies in auditory hair cells from the turtle's papilla.

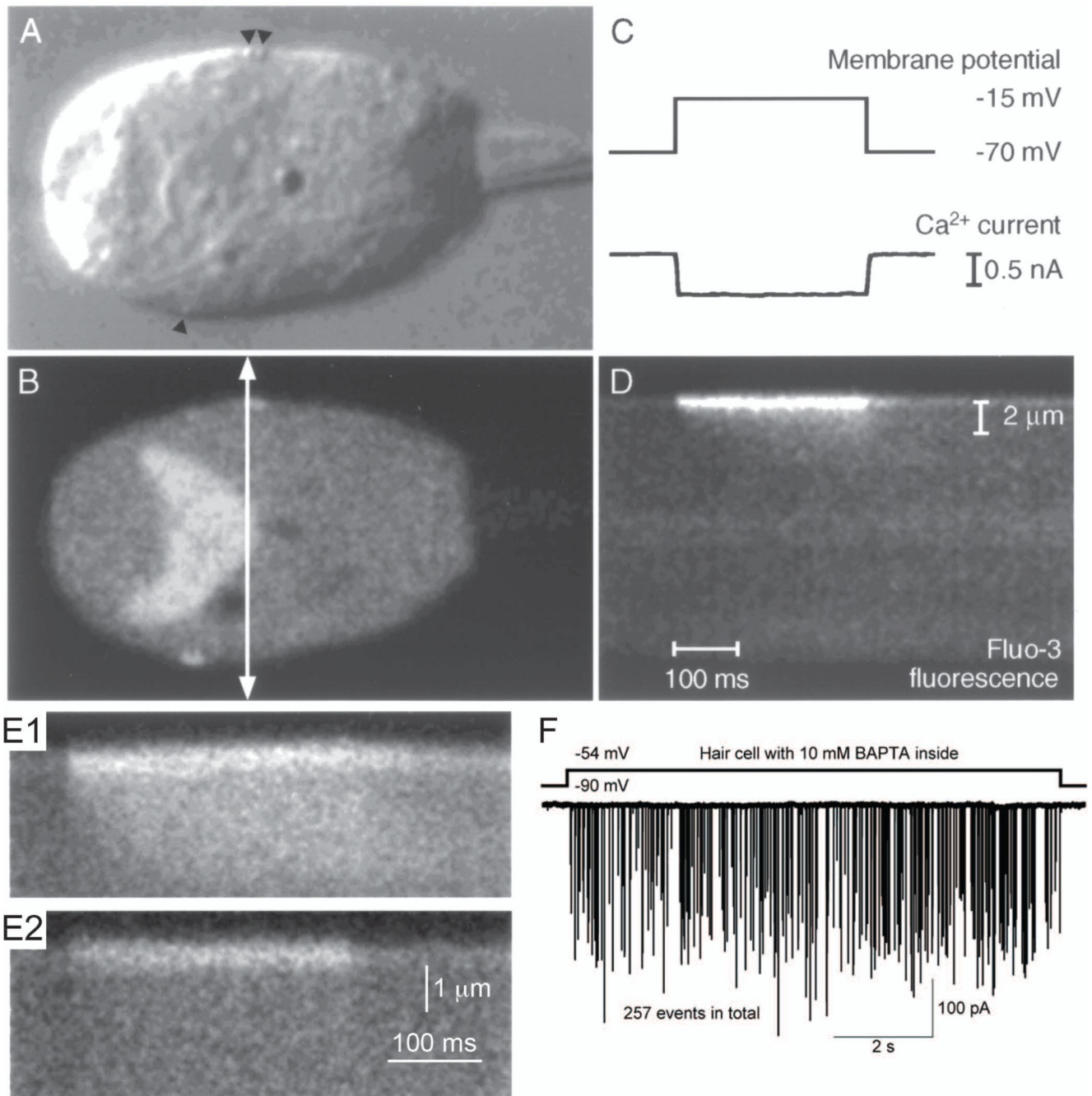
**A.** Fluorescence image of presynaptic dense bodies with rhodamine-tagged ctbp2-terminal binding peptide (scale bar: 1  $\mu\text{m}$ ).

**B.** Regions selected for  $\text{Ca}^{2+}$  imaging.

**C.** A depolarizing stimulus from  $-85$  mV to  $-35$  mV (top) on the hair cell evoked a large L-type  $\text{Ca}^{2+}$  current.

**D.** The fluorescent signal shows a rapid initial increase with subsequent slow rise of the internal  $\text{Ca}^{2+}$  concentration. Regions far from the synapse show little initial response followed by a slow slight increase. This indicates  $\text{Ca}^{2+}$  channels are clustered at the synaptic ribbon sites.

Modified from Schnee et al., 2011[39].

**Figure 3.**

Presynaptic  $\text{Ca}^{2+}$  entry in frog hair cells.

**A.** Image of a hair cell using differential interference contrast light microscopy. Arrowheads indicate the locations of presynaptic ribbons.

**B.** Epifluorescence image of the same hair cell with A, which is loaded with  $200 \mu\text{M}$  fluo-3. The fluorescence image shows strong fluorescence signals at the positions of ribbons. The arrow indicates the transect scanned in D.

**C.** While the image was acquired, the hair cell was depolarized from  $-70 \text{ mV}$  to  $-15 \text{ mV}$  for 300 ms (upper trace).  $\text{Ca}^{2+}$  current was evoked by this stimulus (lower trace).

**D.** Time course of  $\text{Ca}^{2+}$  entry in isolated hair cell loaded with 200  $\mu\text{M}$  fluo-3. The line-scan feature of a laser-scanning confocal microscope with high temporal resolution generated a two-dimensional image. One axis is distance and the other axis is time. A transect (400 nm) across the hair cell (arrow in B) was repeatedly scanned every 2 ms for a period including the depolarization in C. Within a few milliseconds of a depolarization's onset, fluorescence signals increased in restricted region, which was close to the presynaptic membrane, then signals spread gradually to the inside of the cell. The spatial scale bar in D applies to A and B. The temporal scale bar in D applies to C.

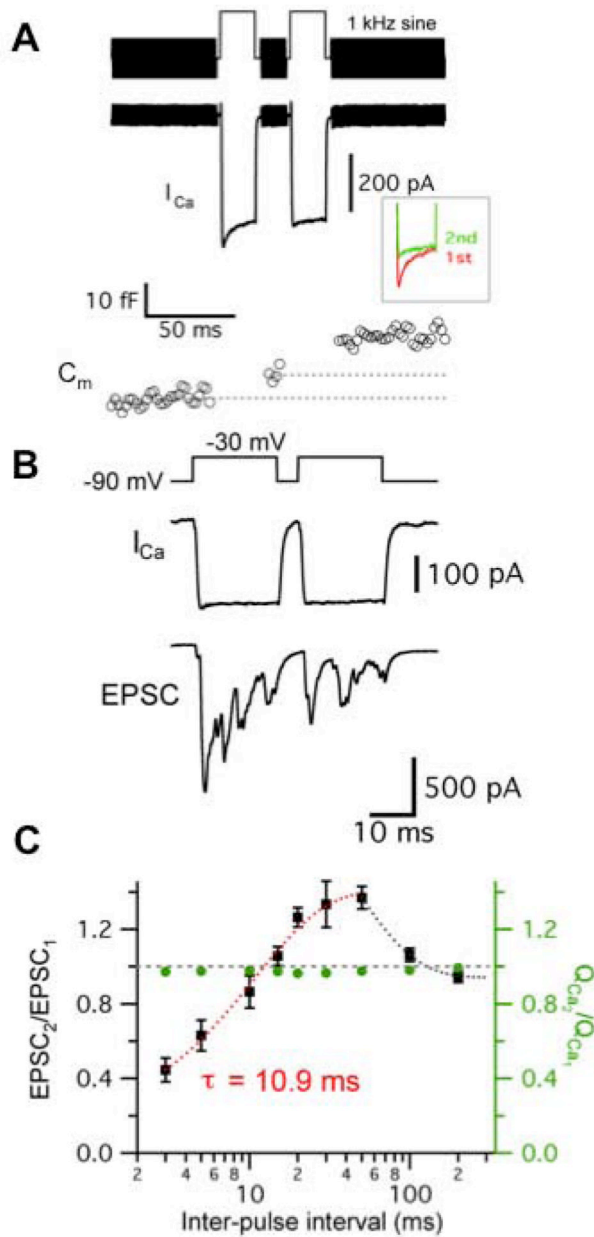
**E.** Mobile  $\text{Ca}^{2+}$  buffer affects temporal and spatial changes in fluo-3 fluorescence. Hair cells were loaded with 200  $\mu\text{M}$  fluo-3 (E1) or 200  $\mu\text{M}$  fluo-3 plus 10 mM BAPTA (E2). The spread of  $\text{Ca}^{2+}$  was restricted to the presynaptic dense body by high concentration of mobile  $\text{Ca}^{2+}$  buffer (E2).

A – E: isolated frog saccular hair cells (modified from Issa and Hudspeth, 1996 [40]).

**F.** EPSCs from paired recordings from the bullfrog amphibian papilla hair cell synapse. Presynaptic hair cell dialyzed with 10 mM BAPTA was depolarized from  $-90$  mV to  $-54$  mV. The afferent fiber shows large amplitude EPSCs during the depolarizing pulse. Modified from Graydon et al., 2011 [6].



Bullfrog amphibian papilla hair cells



Goldfish retina bipolar cells

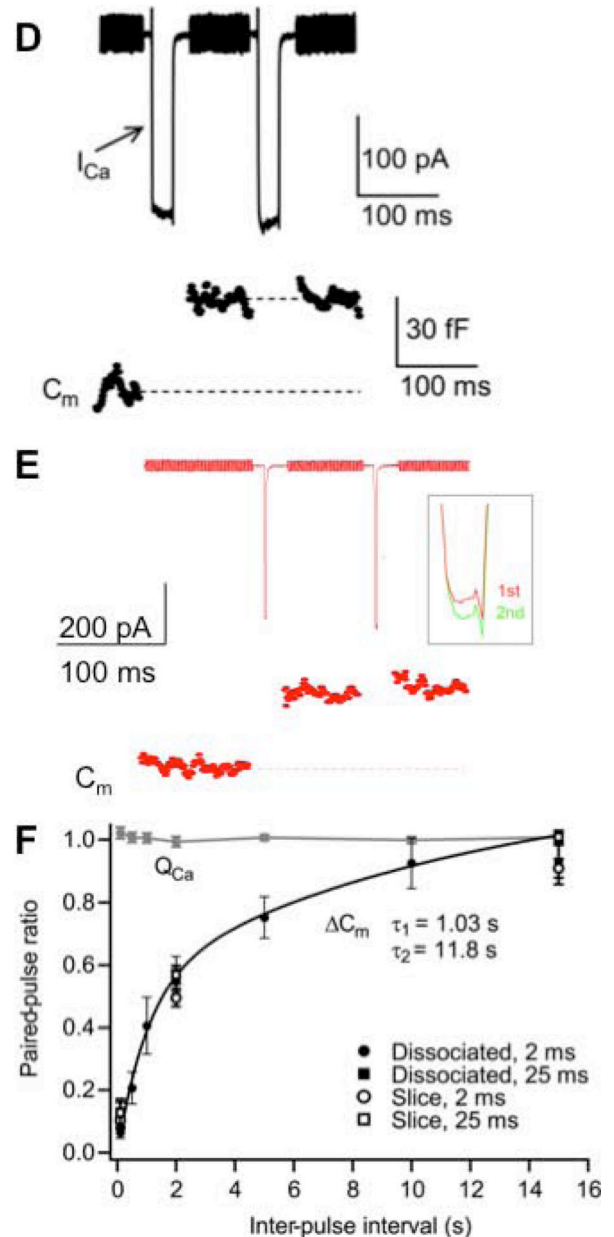


**Figure 4.** Short-term plasticity at bullfrog auditory hair cell synapses (A – C) and goldfish retina bipolar cell synapses (D – F).

**A.**  $\text{Ca}^{2+}$  current ( $I_{\text{Ca}}$ ) and membrane capacitance ( $C_m$ ) evoked by a pair of 20 ms depolarization from  $-90$  mV to  $-30$  mV with 20 ms interpulse interval shows paired-pulse facilitation in the ratio of the  $C_m$  jumps. Note that  $I_{\text{Ca}}$  shows a slow form of calcium-dependent inactivation (inset).

**B.** When a hair cell was depolarized from  $-90$  mV to  $-30$  mV for 20 ms with 5 ms interpulse interval, EPSC was recorded from the connected afferent fiber terminal. The ratio of EPSC ( $\text{EPSC}_2/\text{EPSC}_1$ ) shows paired-pulse depression.



**C.** The relationship between EPSC peak ratios and interpulse intervals. Hair cells were depolarized from  $-90$  mV to  $-30$  mV for 20 ms with various interpulse intervals ( $n = 4 - 8$ ). The EPSC paired-pulse ratio ( $EPSC_2/EPSC_1$ ) recovered exponentially with a single exponential fit from 3 to 50 ms intervals ( $\tau = 10.9$  ms; red dashed curve). The gray dashed line indicates that the ratio is 1 ( $EPSC_2 = EPSC_1$ ). The ratio of  $Ca^{2+}$  charge ( $Q_{Ca2}/Q_S$ ) was relatively constant and close to 1 (0.96 – 0.99).

**D.**  $I_{Ca}$  and  $C_m$  were evoked by a pair of 25 ms pulses from  $-60$  mV to  $-10$  mV with 100 ms interpulse interval in dissociated goldfish retina bipolar cells. The ratio of  $C_m$  shows strong paired-pulse depression.

**E.** A bipolar cell was depolarized by a pair of 2 ms pulses from  $-60$  mV to  $-10$  mV with 100 ms interpulse interval. Note that although  $I_{Ca}$  shows slight calcium-dependent facilitation in amplitude (inset), the ratio of  $C_m$  jumps shows strong paired-pulse depression due to vesicle pool depletion.

**F.** Paired-pulse ratio ( $\Delta C_{m2}/\Delta C_{m1}$ ) and the ratio of  $Ca^{2+}$  charge ( $Q_{Ca}$ ) with pairs of 2 ms or 25 ms pulses in dissociated bipolar cell terminals or terminals in retinal slices. Paired-pulse ratio recovered with fast time constant ( $\tau = 1.03$  s; 43 %) and slow time constant ( $\tau = 11.8$  s; 57 %). The black line is a double exponential fit. Under all conditions, the rates of recovery from depression were similar.

A–C: from Cho et al., 2011 [77], D–E: Modified from Palmer et al., 2003 [109].